RADIATION FROM OPEN ENDED WAVEGUIDE WITH A DIELECTRIC LOADING*

Sergey N. Galyamin†[1], Andrey V. Tyukhtin[1], Stanislav S. Baturin[2], Victor V. Vorobev[1], Aleksandra A. Grigoreva[1]
[1]Saint Petersburg State University, 7/9 Universitetskaya nab., St. Petersburg, 199034, Russia
[2]Saint Petersburg Electrotechnical University "LETI", 5 Pr. Popova, St. Petersburg, 197376, Russia

Abstract

Terahertz radiation is considered as a promising tool for a number of applications. One possible way to emit THz waves is to pass short electron bunch through a waveguide structure loaded with dielectric [1]. In our previous papers, we have analyzed this problem in both approximate [2] and rigorous [3] formulation. However, we have encountered certain difficulties with calculations. In the present report, we are starting to develop another rigorous approach based on mode-matching technique and modified residue-calculus technique [4]. We consider the radiation from the open-ended dielectrically loaded cylindrical waveguide placed inside regular cylindrical waveguide with larger radius. We present structure of reflected and transmitted modes and typical radiation patterns from the open end of larger radius waveguide.

THEORY AND ANALYTICAL RESULTS

Analytical methods for investigation of various waveguide discontinuities have been developed several decades ago [4,5]. Here we apply the modified residue-calculus technique to the case of cylindrical waveguide with uniform dielectric filling and open end placed inside infinite waveguide. In the sequel, we plan to consider layered dielectric filling and perform the limiting process to the case of open-ended waveguide in the free space.

Consider a semi-infinite ideally conducting ($\sigma=\infty$) cylindrical waveguide with radius b filled with a homogeneous dielectric ($\varepsilon>1$) and put in a concentric infinite waveguide with radius $a>b$ (Fig. 1). We suppose that single TM_{0l} mode incidents the orthogonal open end (cylindrical frame ρ,φ,z is used):

$$H_{\omega\varphi}^{(i)}=J_1(\rho j_{0l}/b)e^{-\kappa_{zl}^{(1)}z}, \qquad (1)$$

where $J_0(j_{0l})=0$, $\kappa_{zl}^{(1)}=\sqrt{j_{0l}^2b^{-2}-k_0^2\varepsilon}$, $\operatorname{Re}\kappa_{zl}^{(1)}>0$, $k_0=\omega/c$. The reflected field in the area (1) is

$$H_{\omega\varphi}^{(1)}=\sum_{m=1}^{\infty}B_mJ_0(\rho j_{0m}/b)e^{\kappa_{zm}^{(1)}z}. \qquad (2)$$

Fields generated in areas (2) and (3) can be presented by the following series:

*Work supported by the Grant of the President of Russian Federation (No. 6765.2015.2) and the Grants from Russian Foundation for Basic Research (No. 15-32-20985, 15-02-03913).
† s.galyamin@spbu.ru

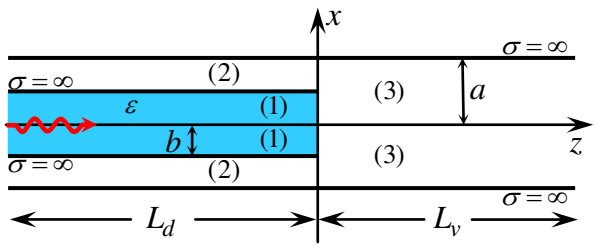

Figure 1: Geometry of the problem.

$$H_{\omega\varphi}^{(3)}=\sum_{m=1}^{\infty}A_mJ_0(\rho j_{0m}/a)e^{-\gamma_{zm}^{(3)}z}, \qquad (3)$$

$$H_{\omega\varphi}^{(2)}=C_0\rho^{-1}e^{\gamma_{z0}^{(2)}z}+\sum_{m=1}^{\infty}C_mZ_m(\rho\chi_m)e^{\gamma_{zm}^{(2)}z}, \qquad (4)$$

$\gamma_{zm}^{(3)}=\sqrt{j_{0m}^2a^{-2}-k_0^2}$, $\gamma_{z0}^{(2)}=-ik_0$, $\gamma_{zm}^{(2)}=\sqrt{\chi_m^2-k_0^2}$, $\operatorname{Re}\gamma_{zm}^{(2,3)}>0$,

$$Z_m(\xi)=J_1(\xi)-N_1(\xi)J_0(a\chi_m)N_0^{-1}(a\chi_m), \qquad (5)$$

χ_m is solution of dispersion relation for area (2),

$$J_0(b\chi_m)N_0(a\chi_m)-J_0(a\chi_m)N_0(b\chi_m)=0. \qquad (6)$$

Performing matching of $H_{\omega\varphi}$ and $E_{\omega\rho}=c(i\omega\varepsilon)^{-1}\partial H_{\omega\varphi}/\partial z$ for $z=0$, and integrating separately over $0<\rho<b$ and $b<\rho<a$, we can obtain the following infinite systems for unknown coefficients:

$$\sum_{m=1}^{\infty}\left(\frac{\tilde A_m}{\gamma_{zm}^{(3)}-\gamma_{zp}^{(1)}}+\frac{\tilde A_mR_p}{\gamma_{zm}^{(3)}+\gamma_{zp}^{(1)}}\right)=\frac{-2\delta_{lp}bJ_1(j_{0p})\gamma_{zp}^{(1)}\kappa_{zp}^{(1)}}{\kappa_{zp}^{(1)}+\varepsilon\gamma_{zp}^{(1)}}, \qquad (7)$$

$$\sum_{m=1}^{\infty}\left(\frac{\tilde A_mR_p}{\gamma_{zm}^{(3)}-\gamma_{zp}^{(1)}}+\frac{\tilde A_m}{\gamma_{zm}^{(3)}+\gamma_{zp}^{(1)}}\right)=\frac{4\tilde B_p\gamma_{zp}^{(1)}\kappa_{zp}^{(1)}}{\kappa_{zp}^{(1)}+\varepsilon\gamma_{zp}^{(1)}}, \qquad (8)$$

$$\sum_{m=1}^{\infty}\frac{\tilde A_m}{\gamma_{zm}^{(3)}-\gamma_{zn}^{(2)}}=0, \quad \sum_{m=1}^{\infty}\frac{\tilde A_m}{\gamma_{zm}^{(3)}+\gamma_{zn}^{(2)}}=-2\tilde C_n\gamma_{zn}^{(2)}, \qquad (9)$$

$\gamma_{zm}^{(1)}=\sqrt{j_{0m}^2b^{-2}-k_0^2}$ $p=1,2,\dots$, $n=0,1,\dots$,

$$R_p=\left(\varepsilon\gamma_{zp}^{(1)}-\kappa_{zp}^{(1)}\right)\left(\varepsilon\gamma_{zp}^{(1)}+\kappa_{zp}^{(1)}\right)^{-1}, \qquad (10)$$

$$\frac{\tilde A_m}{A_m}=J_0\left(\frac{bj_{0m}}{a}\right)\frac{j_{0m}}{a}, \quad \frac{\tilde B_p}{B_p}=\frac{bJ_1(j_{0p})}{2}, \qquad (11)$$

$$\frac{\tilde C_0}{C_0}=\ln\left(\frac{a}{b}\right), \quad \frac{\tilde C_n}{C_n}=\frac{a^2}{2b}\frac{Z_n^2(a\chi_n)}{Z_n(b\chi_n)}-\frac{b}{2}Z_n(b\chi_n). \qquad (12)$$

According to residue-calculus technique [4], to solve systems (7)–(9) one should construct the function $f(w)$

ISBN 978-3-95450-147-2

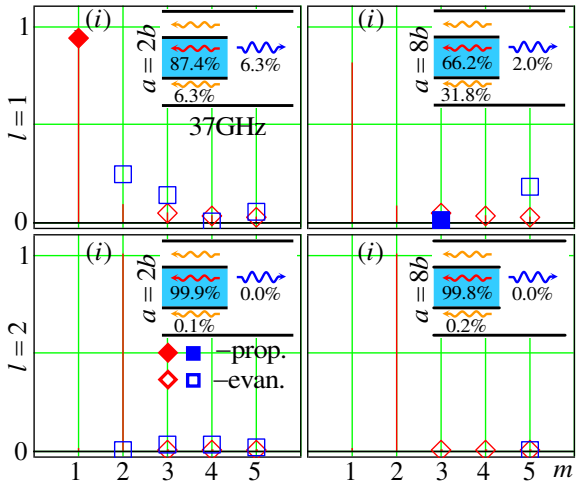

Figure 2: Structure of reflected (red diamonds) and transmitted (blue squares) modes for $b=0.24$ cm, $\varepsilon=10$, $\omega=2\pi\cdot 37$GHz and incident mode with number l. Percent values show total power.

which satisfies the following conditions: (i) $f(w)$ is regular in complex plane w excluding first-order poles $w=\gamma_{zm}^{(3)}$; (ii) has first-order zeros for $w=\gamma_{zm}^{(2)}$; (iii) $f(w)\xrightarrow[|w|\to\infty]{} w^{-(\tau+1/2)}$ with $\sin(\pi\tau)=(\varepsilon-1)/(2\varepsilon+2)$; (iv) $f(w)$ satisfies the relation $f(\gamma_{zp}^{(1)})+R_p f(-\gamma_{zp}^{(1)})=0$ for $p=1,2,\ldots$ excluding $p=l$; (v) and relation

$$f(\gamma_{zl}^{(1)})+R_l f(-\gamma_{zl}^{(1)})=\frac{2bJ_1(j_{0l})\gamma_{zl}^{(1)}\kappa_{zl}^{(1)}}{\kappa_{zp}^{(1)}+\varepsilon\gamma_{zl}^{(1)}}. \qquad (13)$$

Asymptotic (iii) follows from Meixner's edge condition for $\rho=b$, $z\to+0$. It follows from (iv) that $f(w)$ has first-order zeros Γ_m shifted with respect to $\gamma_{zm}^{(1)}$. Considering integrals over circle C_∞ with infinite radius

$$\oint_{C_\infty}\frac{f(w)}{w-\gamma_{zn}^{(2)}}dw=0,\quad \oint_{C_\infty}\left(\frac{f(w)}{w-\gamma_{zp}^{(1)}}+\frac{R_p f(w)}{w+\gamma_{zp}^{(1)}}\right)dw=0, \qquad (14)$$

$$\oint_{C_\infty}\frac{f(w)}{w+\gamma_{zn}^{(2)}}dw=0,\quad \oint_{C_\infty}\left(\frac{R_p f(w)}{w-\gamma_{zp}^{(1)}}+\frac{f(w)}{w+\gamma_{zp}^{(1)}}\right)dw=0, \qquad (15)$$

we obtain $\tilde{A}_m=\mathrm{Res}\, f(\gamma_{zm}^{(3)})$, $\tilde{C}_n=f(-\gamma_{zn}^{(2)})(2\gamma_{zn}^{(2)})^{-1}$,

$$\tilde{B}_p=-\frac{\left(R_p f(\gamma_{zp}^{(1)})+f(-\gamma_{zp}^{(1)})\right)}{4\gamma_{zp}^{(1)}\kappa_{zp}^{(1)}}\left(\varepsilon\gamma_{zp}^{(1)}+\kappa_{zp}^{(1)}\right). \qquad (16)$$

Function $f(w)$ can be constructed in the form

$$f=P_0\frac{(w-\gamma_{z0}^{(2)})\prod_{n=1}^{\infty}\left(1-\frac{w}{\gamma_{zn}^{(2)}}\right)}{\prod_{m=1}^{\infty}\left(1-\frac{w}{\gamma_{zn}^{(3)}}\right)}\prod_{s=1}^{\infty}{}^{(l)}\left(1-\frac{w}{\Gamma_s}\right)G(w), \qquad (17)$$

$$G(w)=\exp\left[-\frac{w}{\pi}\left(b\ln\left(\frac{b}{a-b}\right)+a\ln\left(\frac{a-b}{a}\right)\right)\right]. \qquad (18)$$

Constant P_0 is chosen so that (13) is fulfilled, superscript (l) in (17) means that term with $s=l$ is excluded from corresponding product. Condition (iii) dictates the following asymptotic for Γ_s:

$$\Gamma_s\xrightarrow[s\to\infty]{}\gamma_{zs}^{(1)}+\frac{\pi}{b}\tau\sim\frac{\pi}{b}\left(s-\frac{1}{4}+\tau\right). \qquad (19)$$

Substituting (17) in (iv) and introducing Δ_s so that $\Gamma_s=\gamma_{zs}^{(1)}+\pi\Delta_s/b$, one obtains the following system:

$$\Delta_s=R_s\left(\frac{2b\gamma_{zs}^{(1)}}{\pi}+\Delta_s\right)\prod_{m=1}^{\infty}{}^{(l,s)}\frac{\gamma_{zm}^{(1)}+\gamma_{zs}^{(1)}+\frac{\pi}{b}\Delta_s}{\gamma_{zm}^{(1)}-\gamma_{zs}^{(1)}+\frac{\pi}{b}\Delta_s}\times$$
$$\times\frac{\gamma_{zs}^{(1)}+\gamma_{z0}^{(2)}}{\gamma_{zs}^{(1)}+\gamma_{z0}^{(2)}}\prod_{n=1}^{\infty}\frac{1+\frac{\gamma_{zs}^{(1)}}{\gamma_{zn}^{(2)}}}{1-\frac{\gamma_{zs}^{(1)}}{\gamma_{zn}^{(2)}}}\prod_{q=1}^{\infty}\frac{1-\frac{\gamma_{zs}^{(1)}}{\gamma_{zq}^{(3)}}}{1+\frac{\gamma_{zs}^{(1)}}{\gamma_{zq}^{(3)}}}G^2(-\gamma_{zs}^{(1)}), \qquad (20)$$

$s=1,2,\ldots$, $s\neq l$. System (20) can be solved numerically using iteration process [4]. Condition (19) gives convenient zero-order approximation for Δ_s and simplifying considerably the control of convergence.

NUMERICAL RESULTS

Coefficients of reflected (B_m) and transmitted (A_m) modes calculated using the described approach are shown in Figs. 2 and 3. Figure 2 shows the case of relatively low frequency: in this case dielectric waveguide supports 2 propagating modes while area (3) (wide vacuum waveguide) supports from 1 to 4 propagating modes. In all cases, transmission is very weak. For $l=1$, reflection occurs mainly at mode 1, but second reflected mode is also excited. In this case, transmitted power

$$\Sigma_m^t=\frac{ca^2}{8\omega}\sum_{m=1}^{\infty}J_1^2(j_{0m})|A_m|^2\,\mathrm{Re}\left(i\gamma_{zm}^{(3)}\right) \qquad (21)$$

decreases with an increase in a. For the second incident mode ($l=2$), only reflected mode with $m=l$ is generated and this mode takes almost the whole energy, therefore transmission tends to zero.

Figure 3 shows the case of around 3 times larger frequency and first incident mode, $l=1$. In this case, area (1) supports 5 propagating modes for $\varepsilon=10$ and 3 propagating modes for $\varepsilon=2$. Area (3) supports from 3 to 13 propagating modes. Efficient transition into area (3) takes place for $\varepsilon=2$, it is around 90% and weakly depends on larger waveguide radius a. For $\varepsilon=10$, transmission is around 27% and again practically does not depend on a.

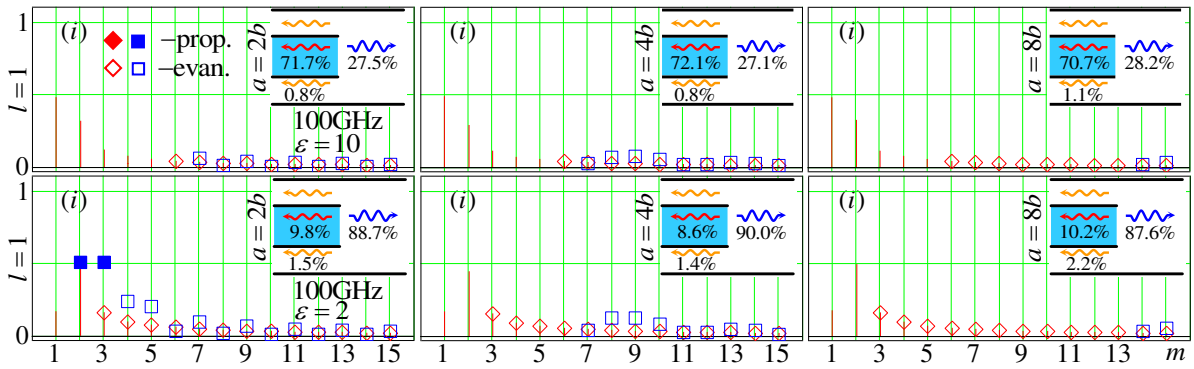

Figure 3. Structure of reflected (red diamonds) and transmitted (blue squares) modes for the first incident mode, $b = 0.24$ cm, $\omega = 2\pi \cdot 100$GHz, $\varepsilon = 10$ (top) and $\varepsilon = 2$ (bottom). Percent values show total power.

For $\varepsilon = 2$ and $\omega = 2\pi \cdot 100$GHz we calculated radiation from the structure by supposing that vacuum area (3) has an open end at distance $L = 3\lambda_{\max}$ ($\lambda_{\max}$ is a wavelength of fastest propagating mode) from the open end of inner dielectric waveguide. We neglected reflection at this end because each mode loses around several percent of its power in this process. We used rigorous formulas [5] and calculated far field using saddle-point technique. Results are shown in Fig. 4.

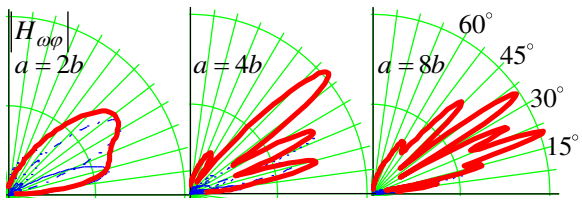

Figure 4. Normalized radiation patterns from the open end of larger radius waveguide. Parameters correspond to lower row in Fig. 3. Blue lines show patterns from first 3 modes as if they were alone.

With an increase in waveguide radius, number of essential lobes in radiation patterns also increases. For the case of 3 modes ($a = 2b$) pattern width is around 45°.

CST SIMULATION

We also simulated mode structure for the case of $\varepsilon = 10$ at 37GHz using CST™ code [6]. Model parameters (Fig. 1) was $L_v = 50$mm, $L_d = 30$mm. We used the time domain solver and calculated powers accepted by 3 non-reflecting ports placed at $z = -15.372$mm in area (1), $z = -30$mm in area (2) and at $z = 50$mm in area (3). We have calculated powers for each simulated mode (we considered 3 axial symmetric modes at each port). Powers going into the corresponding mode coincide with those achieved using our method with 0.7% accuracy (table 1). It should be noted, that calculation performed using our analytical approach take much less time compared with CST code.

In conclusion, we have analyzed transformation of a single TM mode at the open end of cylindrical waveguide with uniform dielectric filling placed inside a larger radius vacuum waveguide. For the case of main incident mode and relatively low permittivity, we have observed that incident power efficiently passes into vacuum waveguide. From $a = 2b$ to $a = 16b$, we haven't observed any significant dependence of transmitted power on the external waveguide radius. On the basis of obtained mode structure, we also have calculated radiation from the open end of vacuum waveguide. For relatively small radius, radiation pattern is wide, while for larger radius patterns contain many narrow lobes comparable with respect to their magnitudes.

Table 1: Power of modes for $a = 2b$, $\varepsilon = 10$ at 37GHz.

Mode (area)	CST	PTC Mathcad 15
1 (1)	87.9%	87.3%
2 (1)	0.1%	0.1%
0 (2)	6.0%	6.3%
1 (3)	6.0%	6.3%
Time	20 min	32 sec

REFERENCES

[1] S. Antipov et al., *Appl. Phys. Lett.*, vol. 100, p. 132910, 2012.
[2] S.N. Galyamin et al., *Opt. Express*, vol. 22, No. 8, p. 8902, 2014.
[3] S.N. Galyamin, A.V. Tyukhtin, A.A. Grigoreva, and V.V. Vorobev, in *Proc. IPAC'15*, pp. 2578-2580.
[4] R. Mittra and S. W. Lee, *Analytical techniques in the theory of guided waves* (Macmillan, 1971).
[5] L. Weinstein, *The Theory of Diffraction and the Factorization Method* (Golem Press, 1969).
[6] http://www.cst.com

ISBN 978-3-95450-147-2